

Special Articles

The Liver Sieve: Considerations Concerning the Structure and Function of Endothelial Fenestrae, the Sinusoidal Wall and the Space of Disse

E. WISSE, R. B. DE ZANGER, K. CHARELS, P. VAN DER SMISSEN AND R. S. MCCUSKEY

Laboratory for Cell Biology and Histology, Free University of Brussels (VUB), Laarbeeklaan 103, 1090 Brussels-Jette, Belgium and the Department of Anatomy, West Virginia University, Morgantown, West Virginia 26506-6302

Sinusoids in the liver lobule (Figure 1) are invested with a unique type of endothelial lining (Figure 2) consisting of endothelial cells with flattened processes perforated by small fenestrae of about $0.1\ \mu\text{m}$ in size (Figure 3). The open fenestrae lack a diaphragm and are arranged in groups to which the name "sieve plates" was given (1). A basal lamina is lacking and for that reason the fenestrae constitute an open connection between the sinusoidal lumen and the space of Disse. It is thought that the major part of the transport and exchange of fluid, solutes and particles between the blood and the space of Disse occurs through these open fenestrae. As a result, obvious filtration effects can be expected when particles of about the size of the fenestrae arrive in the liver. Another unique feature of liver sinusoidal endothelial cells is the high endocytotic capacity, which, together with the fenestrae and the absence of a basal lamina, makes them unique in the body (2). To the best of our knowledge, this particular type of endothelial cell is not found in any other organ. The distinction between endothelial cells and three other types of sinusoidal cells, i.e., Kupffer, fat-storing and pit cells, has repeatedly been described and reviewed (3, 4).

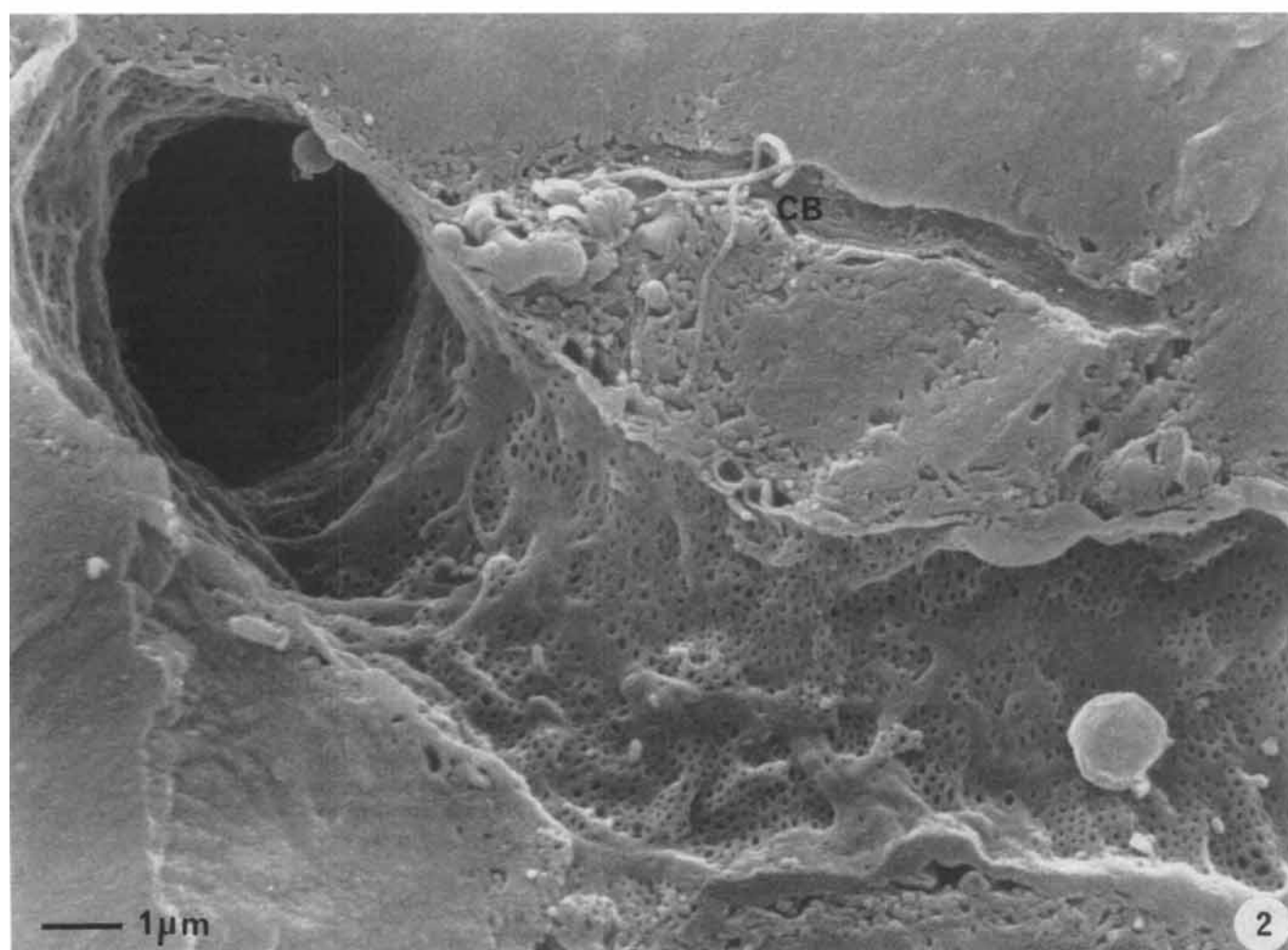
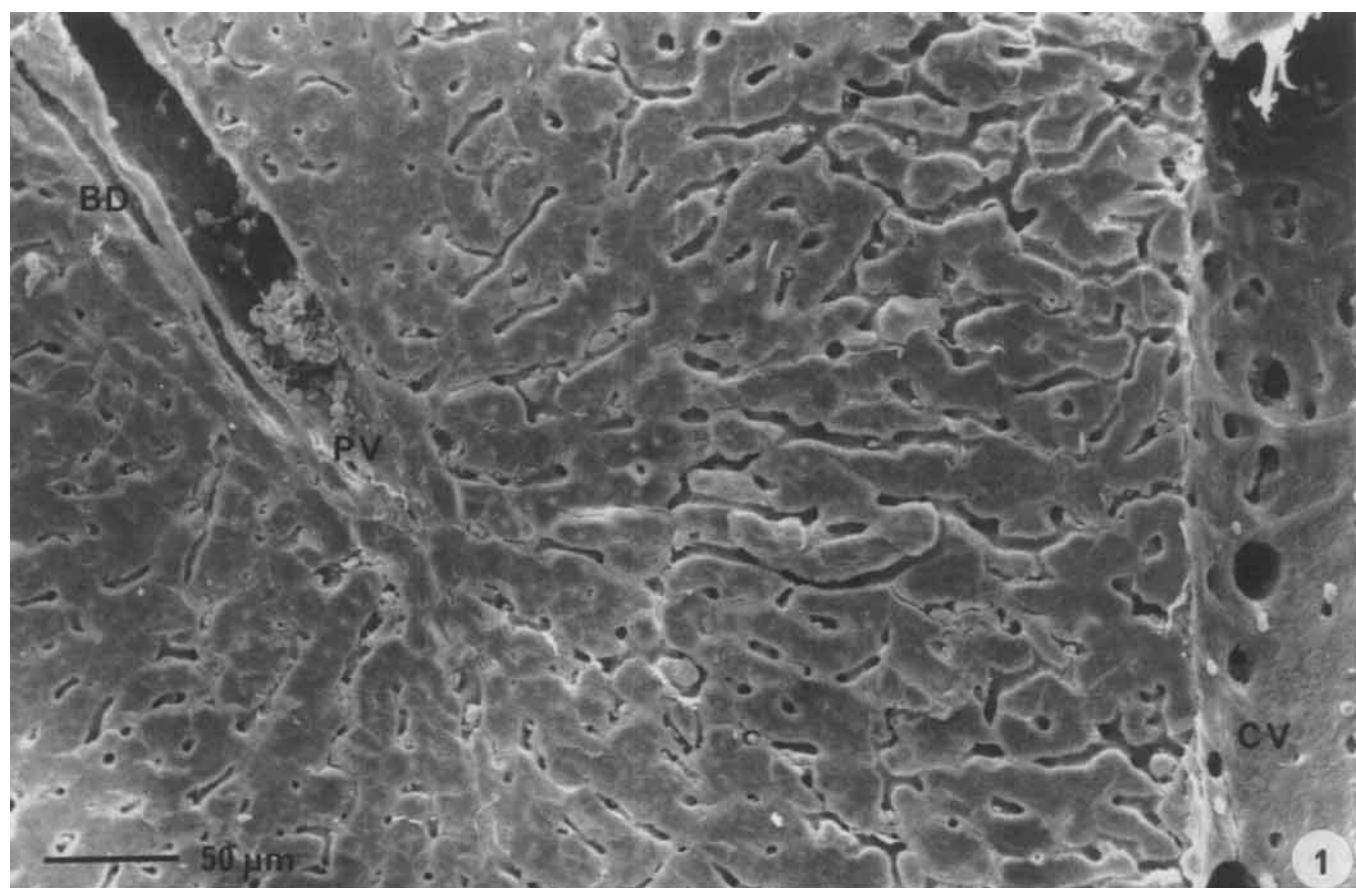
Fenestrae were first observed following perfusion fixation (1); fixation is highly critical in the preservation and visualization of endothelial fenestrae, and this is valid for the sinusoidal area as a whole. No sophisticated apparatus is needed for perfusion fixation of the liver, but successful perfusion fixation is critically dependent on fast and well-dosed anesthesia of relatively stress-free

animals, rapid and adequate surgical procedures and application of low pressure perfusion with the right fixative under proper conditions of temperature, osmolarity, etc. (5). Recently, we described a method of low pressure ($10\ \text{cm H}_2\text{O}$) perfusion fixation for rat liver, which provides good results for the fine structure of the endothelial lining as judged by a low frequency of gaps, i.e., holes larger than the largest fenestrae of 200 to 300 nm (5, 6). Perfusion fixation can be imitated by injection of a fixative into surgical wedge (7) or needle (8, 9) biopsies of liver tissue. Fixation of this type shows a large improvement over immersion fixation, but, in our hands, such material is unsuitable for morphometric evaluation of fenestrae and other sinusoidal structures.

Fenestrae were observed first in ultrathin sections (1) and freeze-etch preparations (1, 10) in the transmission electron microscope (TEM). Later, scanning electron microscopy (SEM) publications showed fenestrae and larger gaps (Figures 4 and 5) (11-14). The frequency distribution of fenestrae follows a Gaussian-like pattern (Figure 6). One might define gaps as holes which represent the tail at the right-hand side of this distribution. Depending on the preparative procedure, the frequency distribution of fenestrae shifts (Figure 6). Plastic embedment reinforces the structures and SEM preparative procedures, due to critical point drying, cause 15 to 30% shrinkage of the tissue. In both cases, however, the shape of the fenestrae frequency distribution curve is largely maintained, permitting differentiation between the population of fenestrae (inside the Gaussian-like curve) and gaps (outside this population). In our SEM preparations, we find a linear relationship between the average diameter of fenestrae of different rat liver preparations and the frequency of gaps (Figure 7); more gaps are found in animals with larger fenestrae (5). So far, the lowest frequency of gaps larger than 200 nm is less than 1%.

This study was supported by Grant 3-0040-80 of the Belgian Fund for Medical and Scientific Research (FGWO).

Address reprint requests to: Dr. E. Wisse, Laboratory for Cell Biology and Histology, Free University of Brussels (VUB), Laarbeeklaan 103, 1090 Brussels-Jette, Belgium.



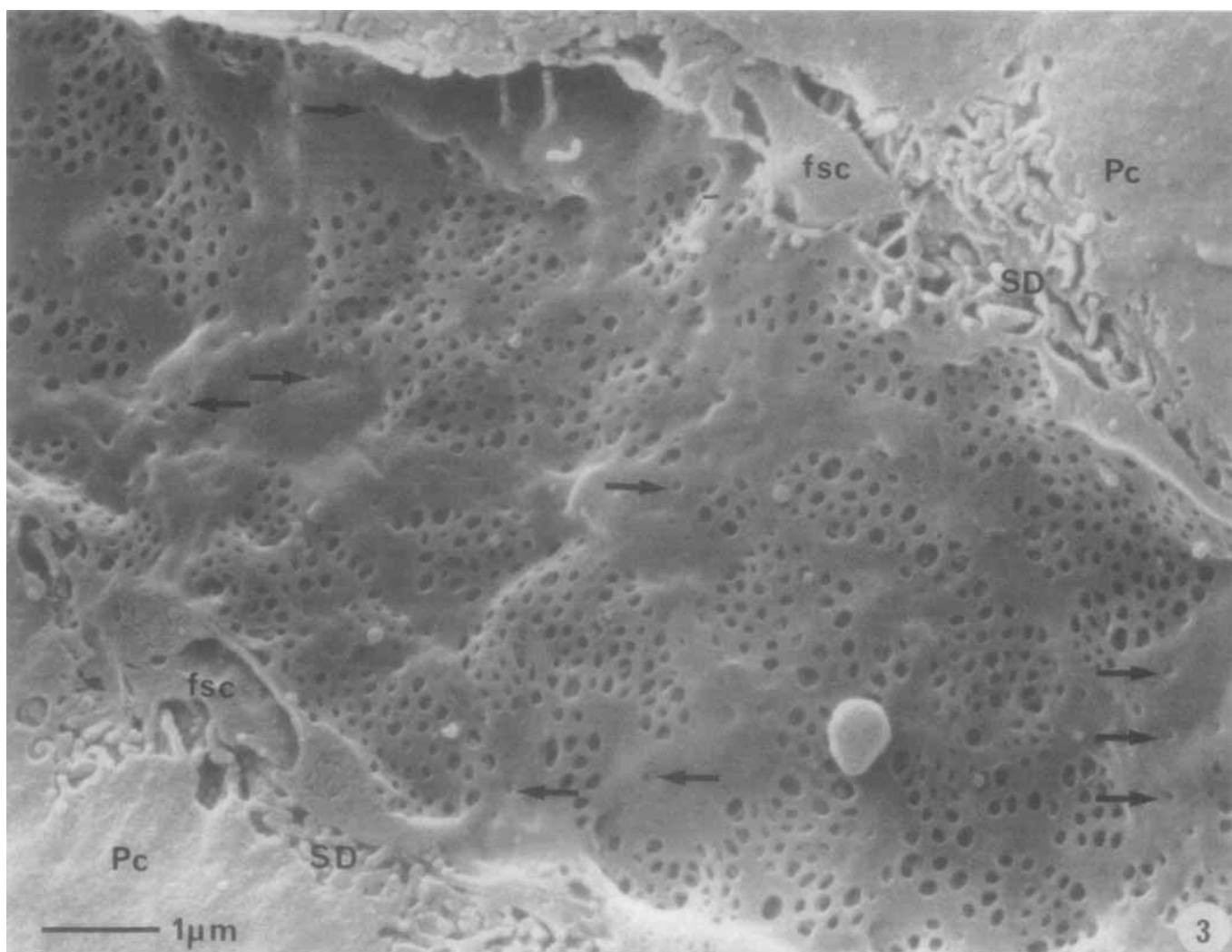


FIG. 3. Higher power SEM micrograph depicting the size differences and clustering of fenestrae in sieve plates. Sieve plates are separated by cytoplasmic arms of endothelial cells, in which depressions of bristle-coated micropinocytotic vesicles (coated pits) can be observed (arrow). In the space of Disse (SD) processes of fat-storing cells (fsc) can be seen. Pc, parenchymal cell with numerous microvilli protruding into the space of Disse.

Gaps occur inter- and intracellularly. Images of fenestrae fusion were recorded (Figure 4) which may explain the possible formation of gaps which have maximum diameters equalling the size of sieve plates. Indirect proof of the artifactual nature of gaps is provided by our attempts to determine what these fenestrae are sieving. In baby rats which drink voluminous amounts of milk from their mothers, chylomicrons or remnants in the space of Disse were never larger than the fenestrae (15). By giving varying intragastric doses of unsaturated corn oil to adult rats, we demonstrated the same filtration effect (6). In both cases, chylomicrons larger than fenestrae remained in the circulation (6, 15). While circulating large chylomicrons (>300 nm) are small in number, their relative volume (as a third power function) may account for 70 to 80% of the total circulating fat. This fraction is obviously not admitted to the space of Disse (6, 15).

However, the smaller, admitted chylomicrons are richer in cholesterol, and their uptake influences the synthesis of cholesterol in the parenchymal cells (16). This suggests a relationship between the fenestrae and the pathogenesis of atherosclerosis. There is little evidence in support of this assumption, however, but a group in New Zealand has recently observed that rabbits have smaller fenestrae than rats (17). The authors relate this phenomenon to the apparent sensitivity of rabbits fed cholesterol to develop atherosclerotic lesions. In contrast, rats which are supposed to more easily clear cholesterol-rich remnants due to their larger fenestrae, do not develop fatty streaks in their vascular wall.

Another possible function of endothelial filtration might be related to the development of acute fatty liver after alcohol consumption. Fenestrae enlarge (18, 19) but decrease in number under the influence of alcohol (19).

FIG. 1. SEM view on a liver lobule. The portal vein (PV) can be recognized because it is associated with a bile duct (BD). Portal veins show infrequent inlet connections to the sinusoids. Sinusoids surrounding the portal vein are rather narrow and tortuous, in centrilobular areas they become wider and straighter. A central vein (CV) is characterized by the presence of many outlet connections with sinusoids.

FIG. 2. SEM picture of a sinusoid, showing the fenestrated wall, the space of Disse and the bordering parenchymal cells. Notice the relative unevenness of the endothelium. CB, collagen bundles.

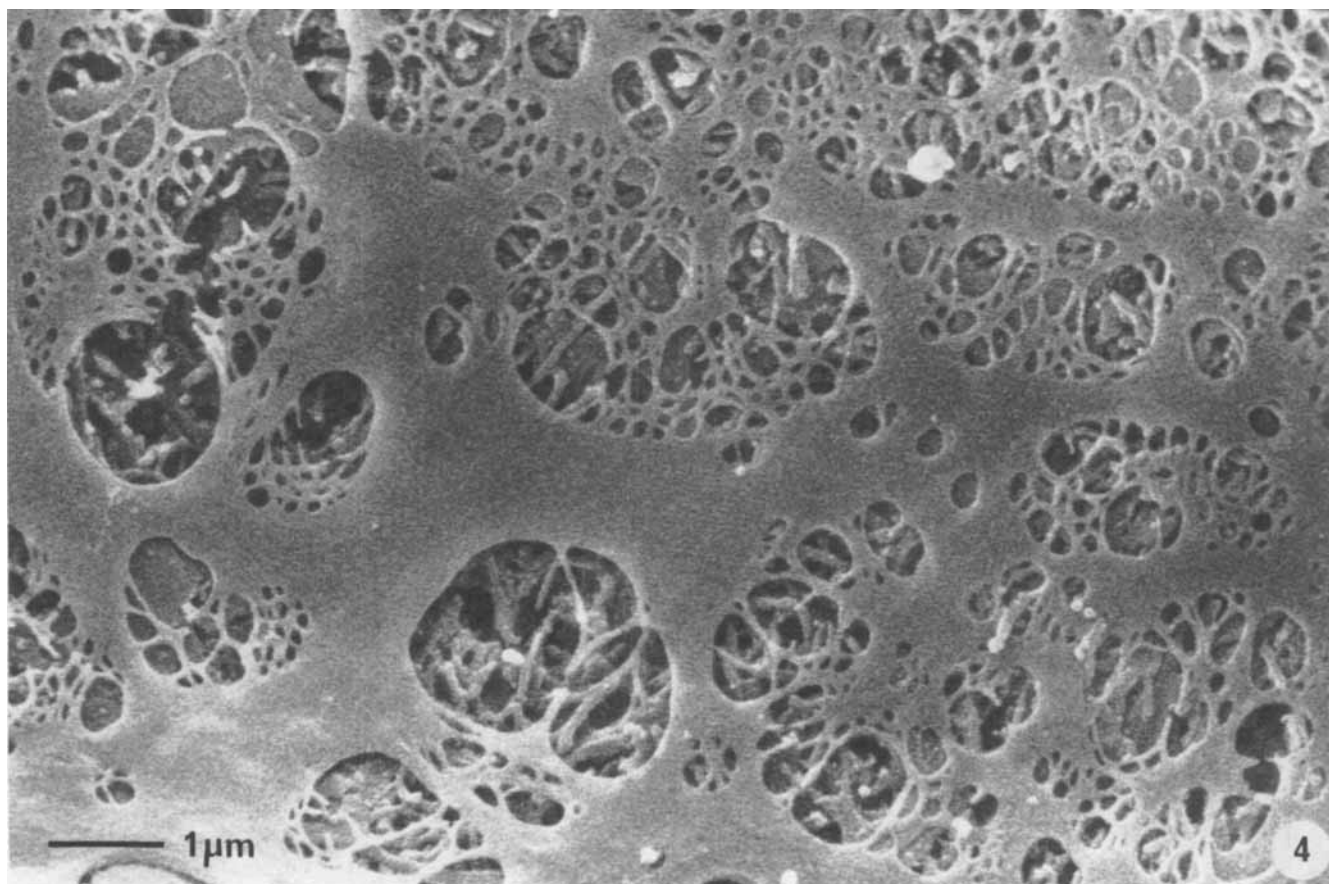


FIG. 4. Gaps originate most probably from the fusion of fenestrae as is suggested by this picture. It is thought that in this sinusoid, perfusion fixation has arrested transitional stages of fenestrae fusion. This results in the formation of gaps, which therefore consists minimally of the fusion of two fenestrae and maximally of all fenestrae in one sieve plate. At the left-hand side of the figure, we find an almost completed gap; at other sieve plates we find fenestrae of normal and more than normal sizes, whereas the small bridges of cytoplasm between fenestrae are thinner than normal (arrows, cf. Fig. 3).

Since the admission of fat to the space of Disse occurs as small particles or droplets, the enlargement of fenestrae may, therefore, contribute to the admission of dietary fat to the parenchymal cells which promotes fatty liver. There also exists a reverse pathway for the transport of lipid, in the form of very low density lipoprotein particles, which assemble in the Golgi apparatus of the parenchymal cell, are transported in vesicles to the sinusoidal cell surface and secreted into the space of Disse. These very low density lipoprotein particles have a size distribution with a maximum of about 90 nm which allows them to pass the endothelial filter (15, 20).

While most studies have been conducted in rodents, fenestrae have been described in a number of other species, including men and other mammalia, birds and fish. Recently, we demonstrated the presence of fenestrae in dog liver, fixed by low pressure (10 cm H₂O) perfusion fixation. Preliminary measurements indicate that the size distribution was almost equal to that of rat liver fenestrae. Fenestrae with diaphragms occur in fetal liver and ruminants (21, 22). A recent report failed to confirm this finding for sheep and goat liver (23, 24). A basal lamina has been reported for sheep liver (25); recent reports indicate that, in goat and sheep, a basal lamina is lacking (23, 24). Nevertheless, strands of basal lamina-like material and collagen type IV (26) are present,

particularly at places where endothelial and fat-storing cell processes are opposed. In CCl₄-treated animals, a basement membrane seems to develop during the onset of cirrhosis (27).

The diameter and frequency of fenestrae differ in periportal and centrolobular areas of the liver lobule. The diameter (as measured in SEM after critical point drying) decreases slightly from 110.7 ± 0.25 nm (S.E.) to 104.8 ± 0.22 nm, whereas the frequency increases from 9 to 13 per μm^2 , resulting in an increase in porosity from 6 to 8% (all figures from periportal to centrolobular) (14) (Figure 6). Measurements made using TEM, reveal periportal and centrolobular fenestrae to measure 174.6 ± 1.0 to 147.2 ± 0.9 nm, respectively. For the SEM preparations, this indicates that critical point drying (CPD) causes a considerable shrinkage at the level of fenestrae (5) (Figure 6). Recently, however, we were able to reduce this CPD shrinkage by applying enforcing techniques by adding tannin to the fixative (GTO method) (28). Preliminary observations indicate that GTO-treated fenestrae are 14% larger than untreated ones due to a reduction in shrinkage during CPD.

Fenestrae are altered by a number of factors *in vivo*. Enlargement of fenestrae diameter has been reported after alcohol (18, 19, 29), pressure (30–32), CCl₄ (29), hypoxia, irradiation and endotoxin (33). Application of

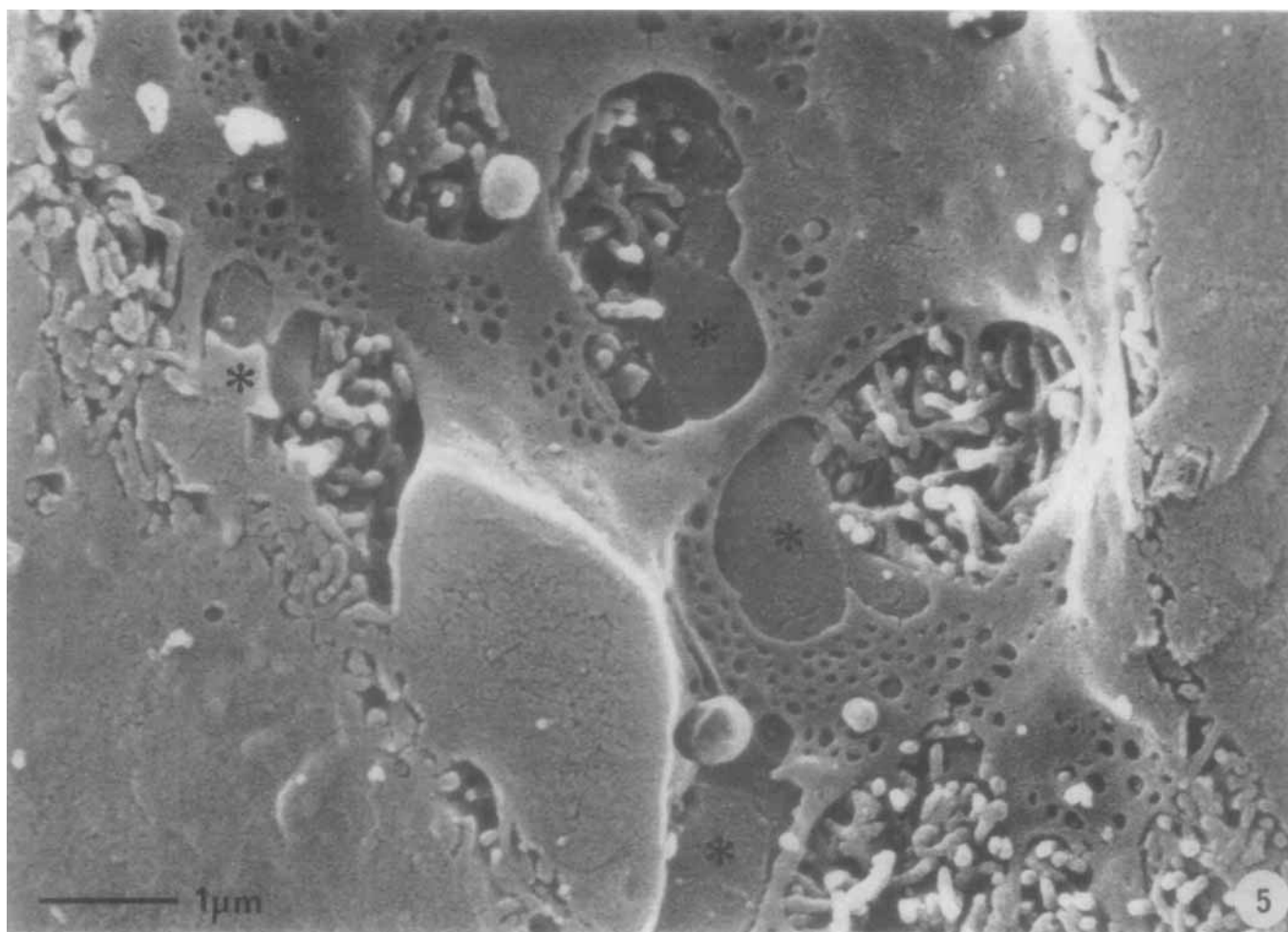


FIG. 5. Endothelial cell with gaps. The presence of gaps enables the observer to look into the space of Disse. In this case, an underlying fat-storing cell (asterisk) can be seen together with microvilli protruding from the parenchymal cell surface.

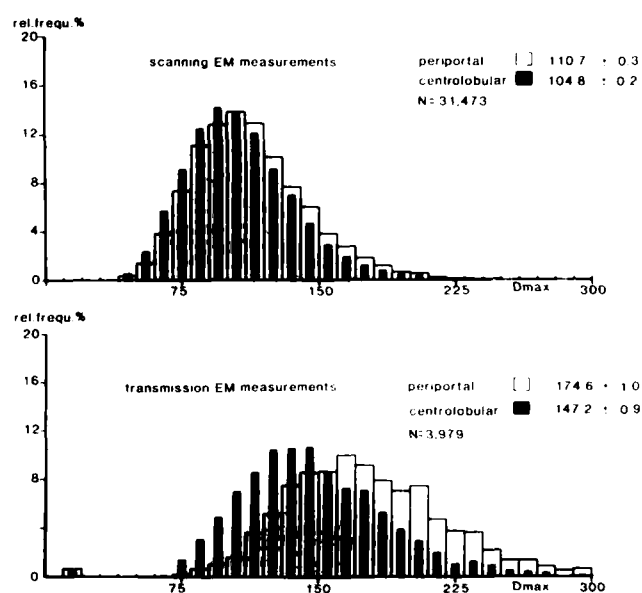


FIG. 6. Size distribution of fenestrae as measured in SEM and TEM. In this material there is a small, but significant difference between periportal and centrolobular fenestrae, the latter being slightly smaller. The difference between SEM and TEM measurements can be explained

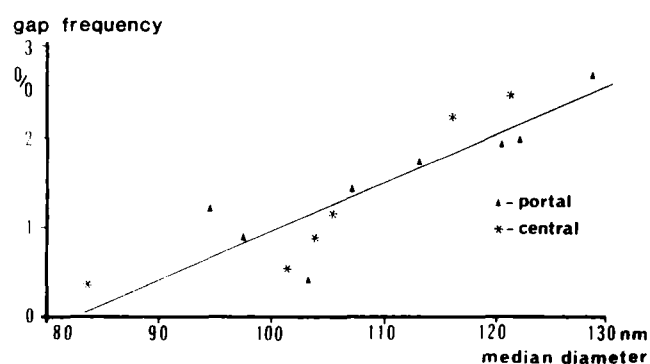


FIG. 7. For 14 populations of periportal and centrolobular fenestrae (seven rats), a relation between gap frequency and median fenestrae diameter was found to be rectilinear with a correlation coefficient of 0.88. This means that more gaps are formed when the population of fenestrae tends to be on the large side. In further trials, we found that larger fenestrae populations have the same shape of size distributions as in Fig. 6. One of the main reasons for this might be the different rates of shrinkage between different experiments.

by the shrinkage of the tissue as a result of CPD, a step in the SEM preparation procedure. In both cases, there is a tail to the *right-hand side* of the distribution curve, indicating the presence of gaps which might be defined as holes larger than $2 \times$ the median diameter.

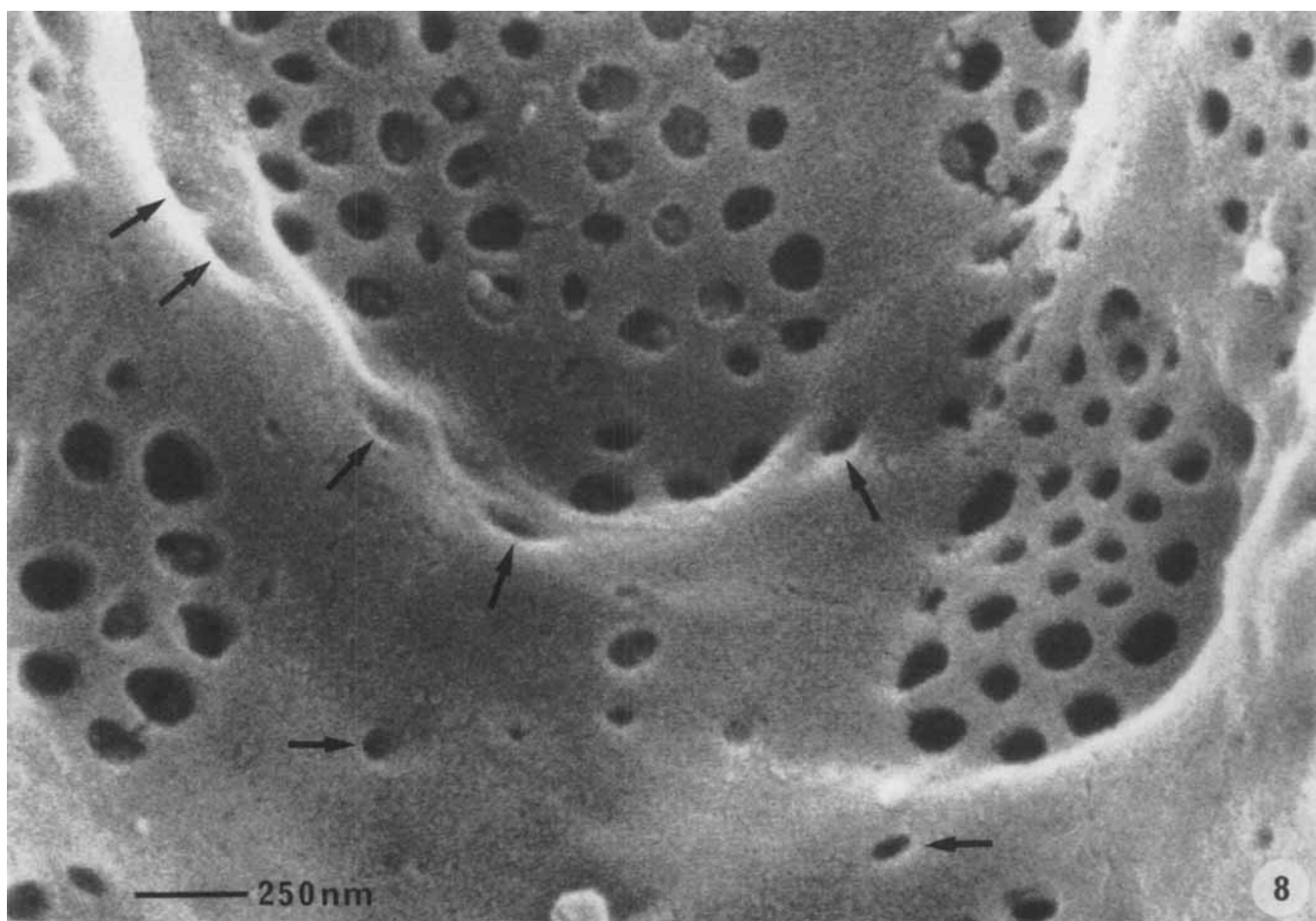


FIG. 8. At high SEM magnification (40,000 \times on the monitor), we can observe small pits, which correspond to the coated pits seen in TEM. These structures have about the same dimensions as fenestrae, and it might very well be that they contribute to the new formation of gaps at the interface between sieve plates and cytoplasmic processes (arrows).

serotonin (34) and noradrenalin (34, 35) also decreased fenestrae diameter. Apart from the dynamics of fenestrae diameter, the kinetics of fenestrae number may also be of interest. A recent report on the effect of alcohol (19) indicates that fenestrae increase in size, but decrease in number. Numbers of fenestrae per square micron vary from 3.3 in baboons (19) to 3.87 to 6.67 (36) or 9.08 to 13.3 (14) in rats. This variation in the reported number and diameter of fenestrae as well as the occurrence of gaps constitutes a big problem in the study of the structure and function of endothelial fenestrae. These problems are related to preparative procedures, and further improvements are required in fixation and reinforcement of the material by preparative techniques, such as treatment with tannin (28). Studying the number of fenestrae per square area may provide interesting data concerning the kinetics of these delicate structures. At the same time, it raises the question as to how these structures are formed and how they might disappear. Although nothing realistic can be said about this aspect, one might speculate that *de novo* formation of fenestrae occurs through micropinocytosis (37) (Figure 8), which, in these cells, is exclusively of the bristle-coated type (2). Reduction in the number of fenestrae may occur either by fusion or extensive constriction and disappearance of fenestrae through membrane fusion. Endothelial cells of sinusoids or capillaries in hyperplastic nodules, developed by treat-

ment with diethylnitrosamine, are reported to lack fenestrations (38). This process of capillarization of sinusoids needs further attention, since it has wide implications for liver function. The cytoskeleton plays a role in fenestrae dynamics and kinetics. From early morphological studies, the presence of cytoplasmic microtubuli and the occurrence of microfilaments in sieve plate areas was obvious (1). Recently, we found actin and myosin filaments in isolated endothelial cells, indicating that contractile proteins may be involved in size changes of fenestrae and sinusoids.

New data on fenestrae are expected from studies on endothelial cells in culture. Knook et al. (39, 40) published a method for the isolation and purification of liver sinusoidal endothelial cells. Steffan et al. (41) and De Leeuw et al. (42) put these cells into culture and maintained them for more than 1 week on collagen-coated substrates. Endothelial cells round up during isolation and internalize their sieve plates. After attachment to the collagen layer, the cells spread out and reexpose their fenestrae. In one experiment, we measured by SEM the size of these fenestrae *in vitro* as 106.6 ± 2.1 nm and found that they still responded to alcohol and serotonin.

Lobular gradients in the frequency and diameter of fenestrae are paralleled by gradients in the morphometry of sinusoids (5, 14). Periportal sinusoids are narrow [$4.0 \mu\text{m} \pm 0.06 \mu\text{m}$ (\pm S.E.) in SEM, $6.42 \pm 0.012 \mu\text{m}$ in light

microscopy, plastic embedding] and more tortuous than centrolobular ones ($5.67 \mu\text{m}$ in SEM and $7.62 \mu\text{m}$ in light microscopy, plastic embedded) (Figure 9, Table 1) (14). *In vivo* microscopic measurements indicate a difference of 5.9 to $7.1 \mu\text{m}$ for a lobular gradient in sinusoidal diameter (Table 1). There is also an increase in the perimeter of sinusoids in centrolobular areas, parallel to the earlier mentioned increase in fenestrae frequency or porosity. These structural parameters favor the possibilities of centrolobular uptake and exchange processes. Many substances are preferentially taken up in periportal regions of the liver lobule (43), but structural param-

eters may partly counterbalance or compensate for preferential periportal uptake.

Our measurements on the size of sinusoids demonstrate that a considerable number of blood cells are actually too large to fit into sinusoids (Table 1). Most published data on the size of different types of blood cells are inaccurate because they are based on measurements on air-dried smear preparations. Studies based on more reliable techniques demonstrate that size distributions of red and white blood cells overlap size distributions of periportal, and to a lesser extent centrolobular sinusoids (Table 1, Figure 9, Refs. 5, 14). We recently observed, by using *in vivo* microscopy (44–47), considerable interaction between blood cells and the sinusoidal wall (Figure 10). Red blood cells pass in a single row and adapt their shape to size differences, obstacles and curves in the periportal sinusoids. White blood cells are less plastic

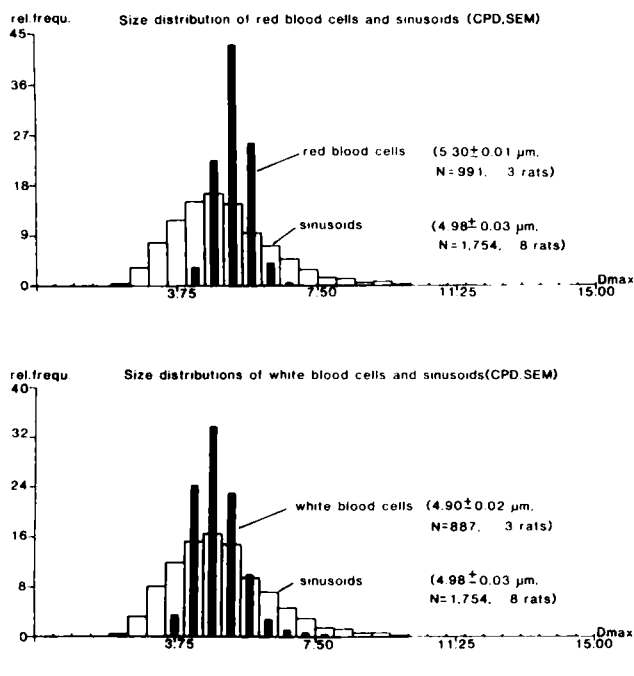


FIG. 9. Size distribution of sinusoids and red and white blood cells, extending the data of Table 1. From these two graphs, one might conclude that starting at $3.75 \mu\text{m}$ blood cells are larger than a certain percentage of sinusoids. At about the size of $7 \mu\text{m}$, white blood cells are bigger than most sinusoids, and these cells will progressively plug sinusoids in the range of approximately $4 \mu\text{m}$ (in SEM preparations).

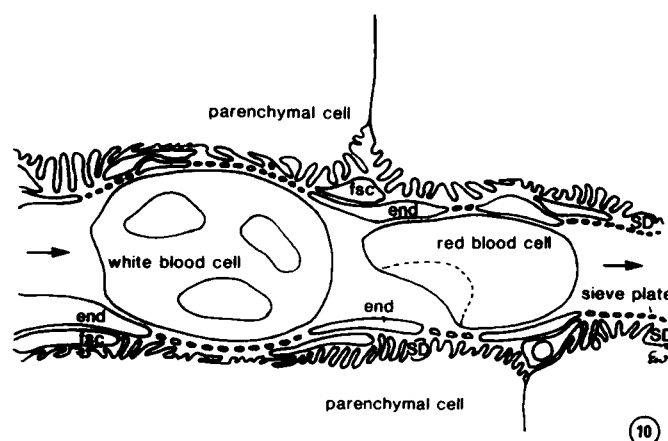


FIG. 10. shows the interaction of blood cells and the fenestrated sinusoidal wall. As observed in the *in vivo* microscope, red blood cells pass by in a single row and show typical deformation morphology. Their observed flexibility is enormous, and in slow streaming sinusoids one observes that red blood cells adapt their diameter constantly to the diameter of the sinusoid by expanding and narrowing. This implies that uptake and exchange is taking place from volumes of plasma in between the red blood cells. White blood cells are much more rigid than red blood cells and are thought to compress the space of Disse, thereby performing endothelial massage (Fig. 12).

TABLE 1. COMPARISON OF MEASUREMENTS ON SINUSOIDS AND BLOOD CELLS IN MICRONS \pm S.E.

	<i>In vivo</i> /LM ^a	<i>In plastic</i> /LM	After CPD/SEM
Portal sinusoid	5.9 ± 0.17 (n = 545, 6 rats)	6.42 ± 0.12 (n = 696, 2 rats)	4.09 ± 0.06 (n = 1, 452, 10 rats)
Central sinusoid	7.1 ± 0.29 (n = 498, 6 rats)	$7.62 \pm \text{ND}^b$ (n = 696, 2 rats)	$5.67 \pm \text{ND}$ (n = 1, 452, 10 rats)
Red blood cells	7.32 ± 0.03 (n = 453, 3 rats)	6.87 ± 0.02 (n = 1, 313, 3 rats)	5.40 ± 0.02 (n = 1, 670, 3 rats)
White blood cells	8.50 ± 0.08 (n = 536, 4 rats)	6.67 ± 0.03 (n = 960, 4 rats)	4.90 ± 0.02 (n = 887, 3 rats)

Comparison of the sizes of sinusoids and blood cells. With three different preparations, such as looking at living or freshly isolated cells and sinusoids *in vivo*, or at plastic-embedded material, or at CPD SEM preparations, it appears that both red blood cells and white blood cells are bigger than periportal sinusoids. This implies deformation of the cells during passage through sinusoids. Due to the occurrence of large white blood cells, such as monocytes or polymorphs, small periportal sinusoids are repeatedly plugged as was confirmed by *in vivo* microscopy.

^a LM, light microscopy.

^b ND, not determined.

and do not easily adapt to obstacles or diameter changes of sinusoids. They interrupt blood flow (44-47) and either change their shape slowly and are pushed out of the sinusoid or attach to the endothelium and migrate by active movement, sometimes against the direction of flow. This peculiar behavior not only causes a high degree of irregularity of periportal blood flow, but also contributed to the function of the fenestrated endothelial lining and the underlying space of Disse. Two new concepts have evolved, based on our measurements and *in vivo* microscopy observations: (a) "forced sieving" (Figure 11) and (b) "endothelial massage" (Figure 12). "Forced sieving" and "endothelial massage" are supposed to promote the transport of particles and fluids into and out of the

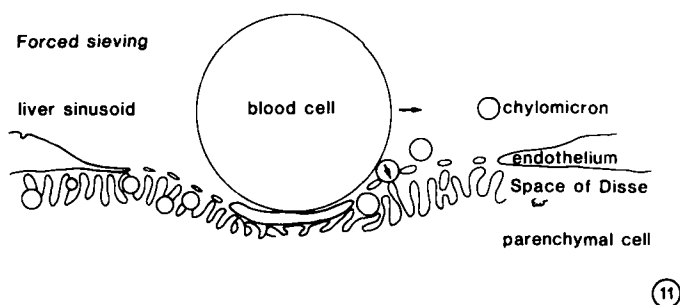


FIG. 11. Diagram of the concept of forced sieving. Soft, fast-moving globular bodies will promote the entrance of fluid or solid phase droplets or particles (lipoproteins) into the space of Disse. These particles are subject to Brownian movement, and blood cells will restrict their movements one-sidedly, thereby enhancing their chance to move to the direction of the space of Disse. When fenestrae are present, particles will "escape" to the surface of the parenchymal cell where they are taken up.

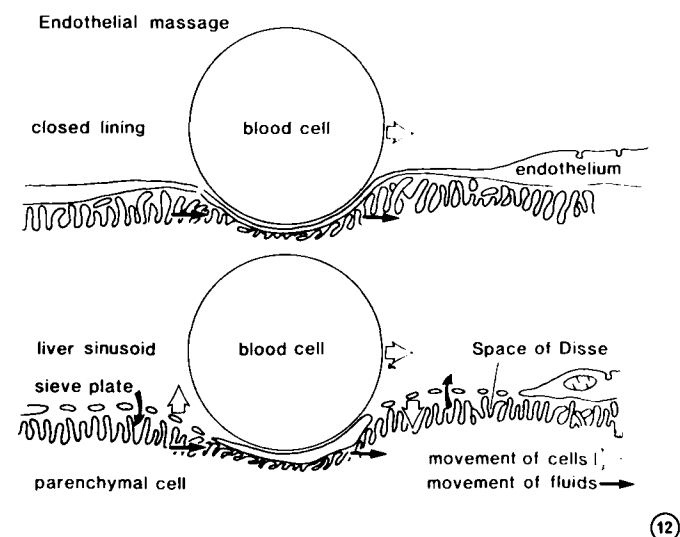


FIG. 12. Diagram of the concept of endothelial massage. One of the effects of compression of the space of Disse by moving white blood cells will be displacement of fluids within this space in a downstream direction. When fenestrae are encountered, fluid will flow out of the space and when white blood cells move along, the microvilli and the endothelial lining will come back into position, and as a result fresh plasma will be sucked into the Disse's space. In *in vivo* microscopy preparations of rat liver, it was seen that white blood cells can retard the flow rate in sinusoids without interrupting blood flow. This retardation is thought to represent an optimal situation for endothelial massage.

Why microvilli on the liver parenchymal cell surface make sense

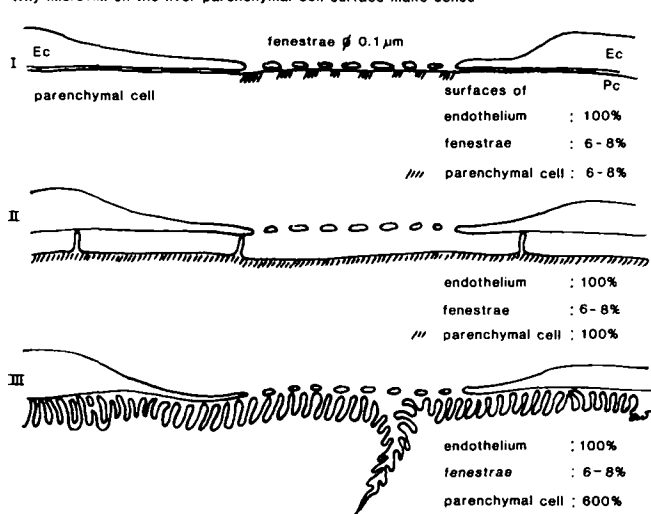


FIG. 13. The depiction of the space of Disse in two hypothetical (I, II) and one realistic conformations (III). Supposing that microvilli are absent (I), the actively exchanging surface of the parenchymal cells (Pc) will be restricted to the part directly in contact with the fenestrae. This surface amounts to 6 to 8% of the endothelial lining (100%). When a few microvilli would maintain a distance between the endothelial filter and the Pc, the total surface of the Pc becomes available for uptake and exchange. The 6 to 8% endothelial porosity might become a limiting factor (II). Microvilli enlarge the Pc surface 6 times. The fenestrae represent a bottle-neck for transport to the enlarged (600%) surface of Pc. This situation asks for special mechanisms of transport, which may be found in concepts such as endothelial massage and forced sieving.

space of Disse, which consists at one side of a thin endothelial layer and at the other side of the plasma membrane of the parenchymal cells. The presence of fenestrae reduces the surface available for free transport to 6 to 8% of the total endothelial surface (14), whereas the parenchymal surface available for uptake is 6.0 times enlarged by microvilli (48). The combination of these facts creates a bottle-neck situation (Figure 13); "forced sieving" and "endothelial massage" may contribute to overcome this problem and may further explain the function of the space of Disse.

Any filtering process will be promoted by large smooth bodies which press on and move along the surface of a filter. It is thought that particles or lipid droplets such as chylomicrons, their remnants and possibly other lipoproteins, are aided to pass the filter due to their interaction with the moving red blood cells. The passage of red blood cells in a single row implies that exchange between the lumen and the space of Disse occurs from small volumes of plasma separated by single cells. The average speed of red blood cells in sinusoids is about 270 to 410 μm per sec, depending on the type of sinusoid, i.e., orientation in the lobule (49). On the basis of our measurements and *in vivo* microscopic observations, we assume that "forced sieving" is more pronounced in periportal areas of the liver lobule.

"Endothelial massage" is based on the effect of white blood cells which pass through sinusoids in a way similar to a baseball in the silk stocking. White blood cells, being larger than sinusoids (Figure 9), will compress the en-

endothelial lining and the underlying space of Disse; as they move, they will "massage" the endothelial lining. As a result, fluid in the space of Disse is pushed downstream and, when fenestrae are encountered, fluid will be flushed out of the Disse's space. After passage of the white blood cells, the space of Disse resumes its original shape, which causes a suction of fresh fluids into the space of Disse. In this way, "endothelial massage" will be more pronounced in periportal areas.

Both concepts start from the axiom that transport and exchange largely follow the route of the open fenestrations. Diacytosis seems to be a wasteful process when open fenestrae are present. Pinocytosis in liver sinusoidal endothelial cells seems to be a well-developed process, which is, however, largely directed to lysosomal digestion (2, 39, 40). Further experiments are needed to find out to what extent "forced sieving" and "endothelial massage" contribute to the vital process of liver uptake and exchange.

Acknowledgments: Writing of this article has been made possible by the technical assistance of Marleen De Pauw, Chris Derom and Roland Jacobs.

REFERENCES

1. Wisse E. An electron microscopic study of the fenestrated endothelial lining of rat liver sinusoids. *J Ultrastruct Res* 1970; 31:125-150.
2. Wisse E. An ultrastructural characterization of the endothelial cell in the rat liver sinusoid under normal and various experimental conditions, as a contribution to the distinction between endothelial and Kupffer cells. *J Ultrastruct Res* 1972; 38:528-562.
3. Ito T. Recent advances in the study on the fine structure of the hepatic sinusoidal wall: a review. *Gunma Rep Med Sci* 1973; 6:119-163.
4. Wisse E, Knook DL. The investigation of sinusoidal cells: a new approach to the study of liver function. In: Popper H, Schaffner F, eds. *Progress in liver diseases*, Vol VI. New York: Grune and Stratton, 1979: 153-171.
5. Wisse E, De Wilde A, De Zanger R. Perfusion fixation of human and rat liver tissue for light and electron microscopy: a review and assessment of existing methods with special emphasis on sinusoidal cells and microcirculation. *Science of Biological Specimen Preparation*, Chicago: SEM Inc AMF O'Hare, 1984: 31-38.
6. De Zanger RB, Wisse E. The filtration effect of rat liver fenestrated sinusoidal endothelium on the passage of (remnant) chylomicrons to the space of Disse. In: Knook DL, Wisse E, eds. *Sinusoidal liver cells*. Amsterdam: Elsevier, 1982: 69-76.
7. Sandström B. Liver fixation for electron microscopy by means of transparenchymal perfusion with glutaraldehyde. *Lab Invest* 1970; 23:71-73.
8. Muto M, Nishi M, Fujita T. Scanning electron microscopy of human liver sinusoids. *Arch Histol Japan* 1977; 40:137-151.
9. De Wilde A, Van Der Spek P, Devis G, et al. On the fixation of needle biopsies of rat liver tissue as a model to study the fine structure of sinusoidal cells. In: Knook DL, Wisse E, eds. *Sinusoidal liver cells*. Amsterdam: Elsevier, 1982: 85-92.
10. Montesano R, Nicolescu P. Fenestrations in endothelium of rat liver sinusoids revisited by freeze-fracture. *Anat Rec* 1978; 190:861-870.
11. Brooks SEH, Haggis GH. Scanning electron microscopy of rat's liver. Application of freeze-fracture and freeze-drying techniques. *Lab Invest* 1973; 29:60-64.
12. Itoshima T, Kobayashi T, Shimada Y, et al. Fenestrated endothelium of the liver sinusoids of the guinea pig as revealed by scanning electron microscopy. *Arch Histol Jap* 1974; 37:15-24.
13. Motta P, Porter KR. Structure of rat liver sinusoids and associated tissue spaces as revealed by SEM. *Cell Tiss Res* 1974; 148:111-125.
14. Wisse E, De Zanger RB, Jacobs R, et al. Scanning electron microscope observations on the structure of portal veins, sinusoids and central veins in rat liver. *Scanning electron microscopy III*. SEM, Inc., AMF O'Hare, Chicago, Illinois, 1983: 1441-1452.
15. Naito M, Wisse E. Filtrating effect of endothelial fenestrations on chylomicron transport in the neonatal rat liver. *Cell Tissue Res* 1978; 190:371-382.
16. Fraser R, Bosanquet AG, Day WA. Filtration of chylomicrons by the liver may influence cholesterol metabolism and atherosclerosis. *Atherosclerosis* 1978; 29:113-123.
17. Wright PL, Smith KF, Day WA, et al. Small liver fenestrae may explain the susceptibility of rabbits to atherosclerosis. *Atherosclerosis* 1983; 3:344-348.
18. Fraser R, Bowler LM, Day WA. Damage of rat liver sinusoidal endothelium by ethanol. *Pathology* 1980; 12:371-376.
19. Mak KM, Lieber CS. Alterations in endothelial fenestrations in liver sinusoids of baboons fed alcohol: a scanning electron microscopic study. *Hepatology* 1984; 4:386-391.
20. Glaumann H, Bergstrand A, Ericsson JLE. Studies on the synthesis and intracellular transport of lipoprotein particles in rat liver. *J Cell Biol* 1975; 64:356-377.
21. Bankston PW, Pino RM. The development of the sinusoids of fetal rat liver: morphology of endothelial cells, Kupffer cells, and the transmural migration of blood cells into the sinusoids. *Amer J Anat* 1980; 159:1-15.
22. Grubb DJ, Jones AL. Ultrastructure of hepatic sinusoids in sheep. *Anat Rec* 1971; 170:75-79.
23. Wright PL, Clemett JA, Smith KF, et al. Hepatic sinusoidal endothelium in goats. *Aust J Exp Biol Med Sci* 1983; 61:739-741.
24. Wright PL, Smith KF, Day WA, et al. Hepatic sinusoidal endothelium in sheep: an ultrastructural reinvestigation. *Anat Rec* 1983; 206:385-390.
25. Gemmell RT, Heath T. Fine structure of sinusoids and portal capillaries in the liver of the adult sheep and the newborn lamb. *Anat Rec* 1972; 172:57-70.
26. Geerts A, Voss B, Rauterberg J, et al. On the distribution of collagen, fibronectin and laminin in the normal rat liver. In: Knook DL, Wisse E, eds. *Sinusoidal liver cells*. Amsterdam: Elsevier, 1982: 209-217.
27. Okazaki I, Tsuchiya M, Kamegaya K, et al. Capillarization of hepatic sinusoids in carbon tetrachloride-induced hepatic fibrosis. *Bibl Anat* 1973; 12:476-483.
28. Murakami T. Tannin-osmium conductive staining of biological specimens for non-coated scanning electron microscopy. *Scanning* 1978; 1:127-129.
29. Fraser R, Bowler LM, De Zanger RB, et al. Agents related to fibrosis, such as alcohol and CCl₄, acutely affect endothelial fenestrae which may cause fatty liver. In: Gerlach U, et al., eds. *Connective tissue of the normal and fibrotic human liver*. Stuttgart: Thieme Verlag, 1982: 159-160.
30. Fraser R, Bowler LM, Day WA, et al. High perfusion pressure damages the sieving ability of sinusoidal endothelium in rat livers. *Br J Exp Pathol* 1980; 61:222-228.
31. Frenzel H, Kremer B, Richter IE, et al. Der Einfluss des Perfusionsdruckes bei der Perfusionsfixation auf die Feinstruktur der Lebersinusoiden. *Transmissions- und Rasterelektronenmikroskopische Untersuchung*. *Res Exp Med* 1976; 168:229-241.
32. Nopanitaya W, Lamb JC, Grisham JW, et al. Effect of hepatic venous outflow obstruction on pores and fenestrations in sinusoidal endothelium. *Br J Exp Pathol* 1976; 57:604-609.
33. Frenzel H, Kremer B, Hücker H. The liver sinusoids under various pathological conditions. A TEM and SEM study of rat liver after respiratory hypoxia, telecobalt-irradiation and endotoxin application. In: Wisse E, Knook DL, eds. *Kupffer cells and other liver sinusoidal cells*. Amsterdam: Elsevier, 1977: 213-222.
34. Wisse E, Van Dierendonck JH, De Zanger RB, et al. On the role of the liver endothelial filter in the transport of particulate fat (chylomicrons and their remnants) to parenchymal cells and the influence of certain hormones on endothelial fenestrae. In: *Proc Basler Liver Week* 1979. London, England: MTP Press, 1980: 195-200.
35. Oda M, Nakamura M, Watanabe N, et al. Some dynamic aspects of the hepatic microcirculation—Demonstration of sinusoidal endothelial fenestrae as a possible regulatory factor. In: Tsuchiya M, et al., eds. *Intravital observation of organ microcirculation*. The Hague: Excerpta Medica Foundation, 1983: 105-138.

36. Oda M, Tsukuda N, Watanabe N, et al. Heterogeneity of hepatic lobule—Some ultrastructural aspects of hepatic microcirculation system. *J Clin Electr Microsc* 1983; 16:5–6.
37. Palade GE, Bruns RR. Structural modulations of plasmalemma vesicles. *J Cell Biol* 1968; 37:633–649.
38. Ogawa H, Itoshima T, Ito T, et al. Absence of Kupffer cells in carcinogen induced liver hyperplastic nodules: demonstration by intravenous injection of indian ink. *Acta Med Okayama* 1983; 37:79.
39. Knook DL, Blansjaar N, Sleyster ECh. Isolation and characterization of Kupffer and endothelial cells from the rat liver. *Exp Cell Res* 1977; 109:317–329.
40. Knook DL, Sleyster ECh. Separation of Kupffer and endothelial cells of the rat liver by centrifugal elutriation. *Exp Cell Res* 1976; 99:444–449.
41. Steffan AM, Lecerf F, Keller F, et al. Isolément et culture de cellules endothéliales de foies humain et murin. *Comp Rend Acad Sci Paris* 1981; 292:809–815.
42. De Leeuw AM, Barelds RJ, De Zanger R, et al. Primary cultures of endothelial cells of the rat liver. *Cell Tissue Res* 1982; 223:201–215.
43. Gumucio JJ, Miller DL. Liver cell heterogeneity. In: Arias I, et al., eds. *The liver: biology and pathobiology*. New York: Raven Press, 1982: 647.
44. McCuskey RS. A dynamic and static study of hepatic arterioles and hepatic sphincters. *Amer J Anat* 1966; 199:455–478.
45. McCuskey RS, Reilly FD, McCuskey PA, et al. “*In vivo*” microscopic studies of the hepatic microvascular system. *Biblio Anat* 1979; 18:73–76.
46. McCuskey RS. *In vivo* microscopy of internal organs. *Prog Clin Biol Res* 1981; 59:79–87.
47. McCuskey RS. The hepatic microvascular system. In: Koo A, Lam SK, Smaje LH, eds. *Microcirculation of the alimentary tract—Physiology and pathophysiology*. Singapore: World Science Publishing Co., 1983: 57–58.
48. Heath T, Wissig SL. Fine structure of the surface of mouse hepatic cells. *Amer J Anat* 1966; 119:97–128.
49. Koo A, Liang IYS, Cheng KK. The terminal hepatic microcirculation in the rat. *J Exp Physiol* 1975; 60:261–266.